

# Work Function Behavior of a Biased C12A7 Electride in Low Temperature Hydrogen Plasmas

A. Heiler,<sup>1,2, a)</sup> R. Friedl,<sup>2</sup> U. Fantz,<sup>1,2</sup> R. Nocentini,<sup>1</sup> and M. Sasao<sup>3</sup>

<sup>1)</sup>Max-Planck-Institut für Plasmaphysik, Boltzmannstrasse 2, D-85748 Garching, Germany

<sup>2)</sup>AG Experimentelle Plasmaphysik, Universität Augsburg, D-86135 Augsburg, Germany

<sup>3)</sup>Organization for Research Initiatives and Development, Doshisha University, 602-8580 Kyoto, Japan

<sup>a)</sup>Corresponding author: [adrian.heiler@ipp.mpg.de](mailto:adrian.heiler@ipp.mpg.de)

**Abstract.** The development of ion sources for NNBI systems at future fusion devices like ITER or DEMO is based on the surface production of negative hydrogen ions. Thus, low work function converter surfaces are mandatory. Besides the state-of-the-art technique of continuous Cs injection during ion source operation, alternative materials are desirable to overcome the drawbacks of volatile Cs coatings. In this work, a C12A7 electride material is studied regarding the work function behavior in a hydrogen and deuterium plasma environment at ion source relevant conditions. The minimum measured work function obtained during the campaign is  $2.9 \pm 0.1$  eV, with an optimization potential to lower values at better vacuum conditions and higher annealing temperatures. Biasing the sample during plasma operation exhibits a strong impact on the work function performance, which is dependent on the polarity and the applied bias potential. The minimum work function obtained for the C12A7 electride used in this experiment is substantially higher than what is achieved with *in situ* caesiation ( $\sim 2$  eV), but the sample has demonstrated promising properties in terms of plasma resilience.

## INTRODUCTION

For the application of neutral beam injectors for heating and current drive at future fusion devices, negative ion sources operating in hydrogen and deuterium and delivering an extracted ion current of several tens of amperes are mandatory [1]. The current development of such sources is based on the surface conversion of atomic hydrogen and positive hydrogen ions, for which a low electron work function of the plasma grid is a key parameter [2]. At present-day facilities, the alkali metal Cs (bulk work function of 2.1 eV [3]) is continuously evaporated during the ion source operation to generate low work function coatings by surface adsorption onto refractory metals. However, the high chemical reactivity and volatility are major drawbacks of *in situ* caesiation: reactions with impurity gases due to the moderate vacuum level of  $10^{-7} - 10^{-6}$  mbar as well as complex redistribution dynamics due to plasma-surface interactions can lead to a depletion of the Cs reservoirs and a deterioration of the plasma grid work function. Hence, the expected high Cs consumption required to provide stable and reliable ion source performance is a major concern regarding long-pulse operation [4], and drives the search for Cs-free alternatives. Since the material requirements for an ion source converter surface are, however, demanding (i. e., machinability and stability at ambient conditions as well as resilience against the plasma load while providing an efficient negative ionization conversion yield), no viable alternative to Cs has been found so far [4, 5, 6, 7].

A promising new candidate possibly fulfilling the requirements for ion source implementation is the C12A7 electride, hereinafter denoted as C12A7:e<sup>-</sup>. It is the first reported electride that is chemically and thermally stable in an ambient atmosphere, since it hosts its anionic electrons in a rigid lattice framework of positively charged Ca-O-Al cages [8, 9]. Dependent on the incorporated electron density  $N_e$  in the crystallographic cages, the C12A7:e<sup>-</sup> material exhibits either semiconducting properties ( $N_e \lesssim 10^{27} \text{ m}^{-3}$ ) or a metal-like behavior ( $N_e \gtrsim 10^{27} \text{ m}^{-3}$ ) [10]. Due to the weakly bound character of the encaged electrons, the pure C12A7:e<sup>-</sup> surface provides an intrinsic low work function of 2.4 eV, which has been reported by Toda *et al.* [11] for cleaned single-crystal samples under ultra-high vacuum (UHV) conditions. However, the C12A7:e<sup>-</sup> surface properties are particularly sensitive to impurities [12] and the surface work function depends strongly on the surface preparation and the vacuum conditions [10, 11, 13]. Consequently, the C12A7:e<sup>-</sup> work function performance has to be investigated under ion source conditions in order to evaluate its potential use as converter surface. First systematic studies are performed at a laboratory experiment, where vacuum and plasma conditions comparable to those close to the converter surface in negative ion sources are provided. The work function of a C12A7:e<sup>-</sup> surface is monitored for varying plasma-on times in hydrogen and deuterium, and the impact of an applied bias potential to the C12A7:e<sup>-</sup> sample during plasma operation is studied. The reported investigations are conducted with a C12A7:e<sup>-</sup> sample supplied from AGC Inc.

## EXPERIMENTAL SETUP

The investigations of the C12A7:e<sup>-</sup> sample are performed at the laboratory experiment ACCesS [14, 15], which is schematically illustrated in Fig. 1. It consists of a cylindrical stainless steel vacuum vessel (15 cm diameter, 10 cm height) and is evacuated by a turbomolecular and roughing pump to a background pressure of  $\sim 10^{-6}$  mbar (limited by Viton O-ring seals). The C12A7:e<sup>-</sup> sample is clamped to a stainless steel sample holder, which is mounted electrically and thermally insulated at the exchangeable bottom plate close to the vessel center and is designed for a maximum heating temperature of 1000 °C. Temperature monitoring both of the sample holder ( $T_{\text{holder}}$ ) and of the sample surface ( $T_{\text{surf}}$ ) is done by K-type thermocouples. Furthermore, monitoring of the background gases is performed with a differentially pumped residual gas analyzer (RGA). Inductively coupled plasmas (ICPs) can be ignited with a planar copper solenoid on top of the chamber, which is separated from it by a Borosilicate glass plate and a grounded Faraday screen. The solenoid is connected via a matching network to a radio frequency (RF) generator (27.12 MHz with 600 W maximum output power). In this work, hydrogen (H<sub>2</sub>), deuterium (D<sub>2</sub>) and argon (Ar) plasmas are generated with a gas supply from calibrated flow meters. Plasma parameters such as the electron temperature, electron density and atomic hydrogen density can be determined via a Langmuir probe and via optical emission spectroscopy [14].

The absolute work function of surfaces mounted at the sample holder is measured *in situ* by means of the photoelectric effect. The broadband radiation of a 100 W high pressure mercury lamp in combination with a set of interference filters is used and collimated onto the sample surface via two quartz lenses (see Fig. 1). For each applied interference filter (10 nm full width at half maximum with central wavelengths between 239 and 852 nm), the transmitted mean photon energy  $\langle h\nu \rangle$  is determined by using an absolutely calibrated high resolution spectrometer ( $\langle h\nu \rangle = 5.04 - 1.45$  eV). The respective irradiated power onto the sample is measured with a radiant power meter, giving values between 0.1 – 1 mW. The photoemitted electrons are drawn to the grounded vessel walls with a bias of –30 V, and the respective current is monitored with a Keithley 6487 picoammeter. With the use of a shutter in the optical path, the energy resolved absolute photocurrents  $I_{\text{ph}}(\langle h\nu \rangle)$  are determined by the subtraction of the dark current ( $10^{-11}$  A in vacuum and  $10^{-10}$  A after plasma). Due to the required bias voltage, work function measurements are performed during plasma-off phases.

An accurate determination of the surface work function  $\chi$  from the photoelectric response measurements can be obtained by the application of extrapolation techniques near the work function threshold ( $h\nu \geq \chi$ ). A common method is a fitting routine according to the Fowler theory, after which [16]

$$I_{\text{ph,u}}(h\nu) \propto T_{\text{surf}}^2 f\left(\frac{h\nu - \chi}{k_{\text{B}} T_{\text{surf}}}\right), \quad (1)$$

with  $I_{\text{ph,u}}$  being the photoelectric current per unit incident light intensity,  $f$  being the universal Fowler function and  $k_{\text{B}}$  denoting the Boltzmann constant. Since the Fowler theory is only valid for metallic surfaces, however, the more general power law [17]

$$I_{\text{ph,u}}(h\nu) \propto (h\nu - \chi)^n \quad (2)$$

can be used for the extrapolation to zero photocurrent. The exponent  $n$  depends on the excitation and escape mechanisms involved, and for  $n = 2$ , the Fowler limiting case for  $T_{\text{surf}} = 0$  K is obtained [16]. For semiconducting or adsorbate-covered surfaces, the  $n$ -parameter is typically in the range of 3 – 4 [17, 18].

## RESULTS AND DISCUSSION

The C12A7:e<sup>-</sup> sample (30 mm diameter, 2 mm thickness) from AGC Inc. has a protective layer on its surface and is stored in atmospheric air prior to the measurements. After the installation at the ACCesS experiment, the vacuum chamber is pumped out to a background pressure of  $5 \times 10^{-6}$  mbar, which leads to a residual gas flux of  $\sim 10^{19}$  m<sup>-2</sup>s<sup>-1</sup> (mainly water vapor). The measured work function before any treatment of the electrified is in the range of  $\sim 5$  eV.

### Initial vacuum heat treatment

The C12A7:e<sup>-</sup> sample is heated in vacuum to thermally desorb the surface protective layer and be activated. The temperature of the sample holder is increased incrementally ( $\Delta T \approx 100$  °C) from room temperature up to 850 °C, and

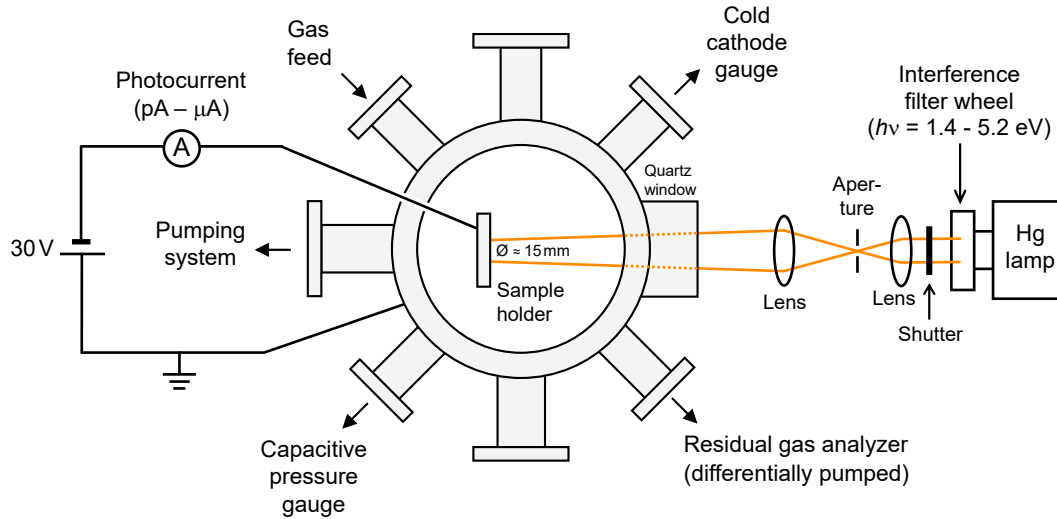


**FIGURE 1.** Schematic of the ICP experiment from top view, including the arrangement of the work function diagnostic setup.

the work function is measured at each temperature step. For a sample surface temperature higher than  $100^{\circ}\text{C}$ , the recorded photocurrents start to increase and the measured work function simultaneously decreases. Continuous RGA monitoring indicates thermal impurity desorption by peaks in the signals for  $\text{H}_2$ ,  $\text{H}_2\text{O}$ ,  $\text{N}_2/\text{CO}$ ,  $\text{O}_2$ , and  $\text{CO}_2$ , which is accompanied by a temporal increase of the background pressure. The work function reaches a value of  $\sim 3.8\text{ eV}$  for surface temperatures  $\gtrsim 480^{\circ}\text{C}$ .

While the measured temperature of the sample holder is  $850^{\circ}\text{C}$  at its maximum, the maximum measured temperature on the sample surface is  $570^{\circ}\text{C}$ . Such a high temperature difference is assumed to be the result of a bad thermal contact between the sample and the sample holder. The minimum measured work function of  $\sim 3.8\text{ eV}$  presumably results from the limited vacuum conditions in combination with  $570^{\circ}\text{C}$  being probably too low for full desorption of the protective layer. When the sample cools down, the photoelectric currents and the work function show a quick deterioration (about  $+1\text{ eV/h}$ ). A work function of  $\sim 4.9\text{ eV}$  is measured the next day.

## Hydrogen and deuterium plasma exposure

Discharges in  $\text{H}_2$  and  $\text{D}_2$  are ignited with an absolute gas pressure of  $10\text{ Pa}$  and an RF output power of  $250 - 300\text{ W}$ . With these operational parameters, electron densities of  $\sim 5 \times 10^{16}\text{ m}^{-3}$  and electron temperatures of  $\sim 2\text{ eV}$  are provided both in  $\text{H}_2$  and  $\text{D}_2$  [15], which mimics the conditions close to the plasma grid in present-day test facilities for fusion [19]. As can be seen in Fig. 2, an initial  $\text{H}_2$  plasma pulse of 5 min leads to an instant reduction of the work function from  $\sim 4.9\text{ eV}$  to  $\sim 3.5\text{ eV}$  without active heating of the sample. Further plasma-on time of more than one hour lowers the work function to  $3.2 \pm 0.1\text{ eV}$ . In steady-state, the hydrogen plasma exposure leads to an elevated surface temperature of  $270^{\circ}\text{C}$ .

As soon as the plasma is switched off, the work function increases with a rate of about  $+0.4\text{ eV/h}$ . The work function deterioration is most likely the result of residual gas adsorption on the  $\text{C12A7:e}^-$  surface and can be reversed by the application of a short plasma pulse ( $\sim\text{min}$ ). Since in the case of a short plasma pulse the sample surface temperature increases only by a few  $10^{\circ}\text{C}$ , thermal effects are negligible and the work function improvement can primarily be ascribed to the pure plasma-surface interaction, i.e., bombardment of the surface with positive ions (mainly  $\text{H}_3^+/\text{D}_3^+$  with energies up to  $10\text{ eV}$ ), atomic hydrogen/deuterium ( $550\text{ K}$  gas temperature), and (V)UV photons (energy range of  $3 - 15\text{ eV}$ ).

The work function of  $3.2\text{ eV}$  is substantially higher than the literature value of  $2.4\text{ eV}$  [11], which indicates that some sort of impurities probably exist on the  $\text{C12A7:e}^-$  surface after the applied hydrogen plasma pulses. Thus, in order to enhance the surface desorption and/or sputtering of the possibly existing impurities, an Ar plasma with  $200\text{ W}$  RF power and  $10\text{ Pa}$  gas pressure is applied for 25 min in total. To reinforce the argon ion bombardment, the sample holder is biased at  $-20\text{ V}$  to ground, leading to a current of  $440\text{ mA}$  and a sample surface temperature of

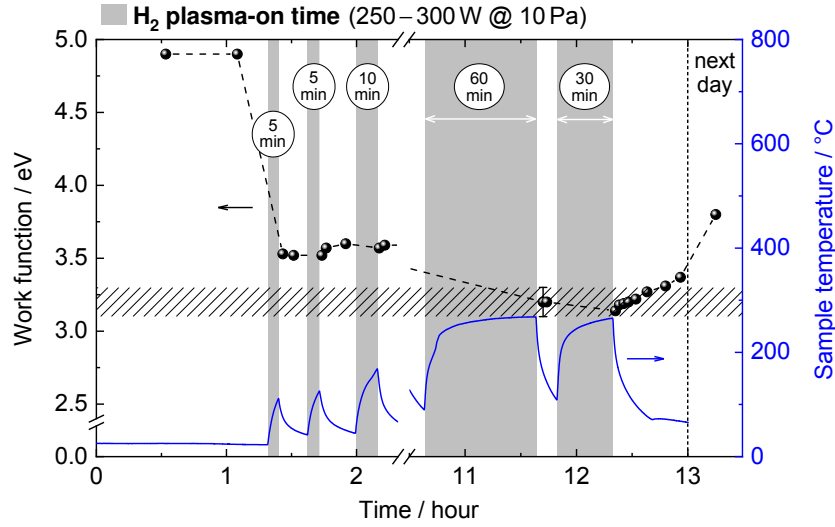


**FIGURE 2.** Influence of hydrogen plasma pulses on the surface work function of the C12A7:e<sup>-</sup> sample. The recorded sample surface temperature is additionally plotted (no active heating applied).

425 °C in maximum. It is observed that the measured work function increases with increasing Ar plasma-on time and the photoemitted currents decrease by more than two orders of magnitude, which might be due to adsorbed Ar at the surface. Finally, the work function reaches a value of higher than 4 eV after argon plasma exposure. With subsequent D<sub>2</sub> plasma pulses, the work function can be reduced again, but reaches still a value not lower than 3.2 eV.

In order to promote a possible synergistic benefit of thermal effects and the plasma-surface interaction, the sample is actively heated up to  $T_{\text{surf}} = 480$  °C during plasma exposure. However, the photoelectric yield decreases with the temperature increase and the work function rises up to  $\sim 3.8$  eV. When the active heating is switched off, a work function of 3.2 eV is retrieved.

### Biasing during plasma exposure

Without the application of an external bias potential, the insulated C12A7:e<sup>-</sup> sample is at its floating potential in the plasma environment, i.e., the total flux of electrons  $\Gamma_e$  towards the entire sample holder surfaces including the C12A7:e<sup>-</sup> surface equals the total flux of positive ions  $\Gamma_+$ . The negative ion flux is assumed to be below 10% and is thus neglected in this consideration. The difference between the floating and plasma potential is about 10 V for both H<sub>2</sub> and D<sub>2</sub> discharges. It is observed that biasing the sample to ground has a substantial influence on the photoemissive properties and the work function behavior of the C12A7:e<sup>-</sup> surface. As can be seen in Fig. 3 a), an applied positive bias potential during D<sub>2</sub> plasma exposure promotes a work function reduction, while a negative bias results in a work function increase (0 V active bias corresponds to the floating potential). Furthermore, the more negative the applied bias potential, the larger the increase of the work function and the associated decrease of the photoelectric currents. An application of  $-60$  V to ground for 15 min results in a work function of  $\sim 3.8$  eV ( $\Delta\chi = +0.6$  eV), and the photoemitted currents are more than one order of magnitude lower than with zero bias. In H<sub>2</sub>, a similar effect is observed, albeit less pronounced ( $\Delta\chi = +0.3$  eV with  $-60$  V bias).

The bias investigations indicate that the C12A7:e<sup>-</sup> surface is sensitive to the flux ratio of positive ions to electrons. When a negative bias is applied, the flux ratio  $\Gamma_+/\Gamma_e$  is  $> 1$ , and a current of 110 mA flows at  $-60$  V. Since this results in a substantial increase of the work function, it is suggested that the anionic electron density in the C12A7:e<sup>-</sup> surface cages is reduced and an electron-deficient surface layer is built up. If this is the case, a depletion of the so-called cage conduction band (CCB) [20] occurs, which is inevitably accompanied with a lowering of the Fermi level. Additionally, surface cage deformations [12] due to an enhanced ion bombardment may also play a role. By the application of a positive bias potential,  $\Gamma_+/\Gamma_e$  is  $< 1$ , and a bias current of 250 mA is associated with a bias potential of  $+20$  V. Here, the work function is decreased, which supports the suggestion that in this case, the electron occupation of the CCB is filled up to a certain extent.

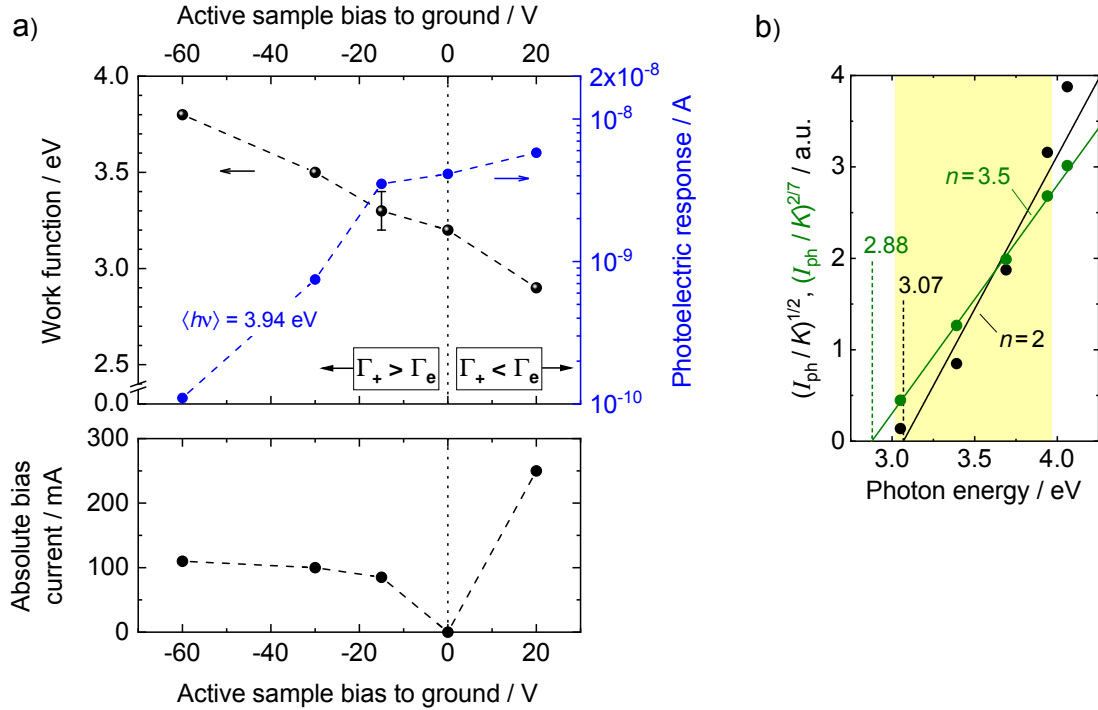


**FIGURE 3.** a) Influence of the application of a bias potential on the C12A7:e<sup>-</sup> surface work function during D<sub>2</sub> plasma exposure (300 W RF power and 10 Pa gas pressure). The respective impact on the photoemitted currents from the surface is exemplarily shown for an irradiated mean photon energy of 3.94 eV. Furthermore, the measured current due to the applied bias voltage is depicted. b) Evaluation of the work function via the threshold of the measured photoelectric response according to Eq. (2): the extrapolation of the photocurrents is illustrated for  $n = 2$  (Fowler limiting case) and for  $n = 3.5$ . The fitting range for the performed linear regression is indicated by the yellowish shaded area.

In Fig. 3 b), the work function evaluation from the measured photoelectric currents after the application of +20 V is exemplarily shown. The photocurrents are evaluated according to Eq. (2):  $(I_{ph}/K)^{1/n}$  is plotted as a function of the photon energy, with  $K$  being the filter dependent relative intensity of the irradiated power, and the extrapolation of a linear least-squares regression is performed. As can be seen, a fit according to the Fowler limiting case for  $T_{surf} = 0$  K, i.e.,  $n = 2$ , leads to a work function of 3.07 eV. However, it does not match the progression of the photocurrents well. By increasing the  $n$ -parameter to 3.5, the fit is significantly improved and yields a work function of 2.88 eV. A similar behavior has already been observed with a different C12A7:e<sup>-</sup> sample [21] and might be the result of a semiconducting surface state of the electride. According to the analysis shown in Fig. 3 b), the work function evaluation is performed with  $n = 3.5$ . With this, a work function minimum of  $2.9 \pm 0.1$  eV is determined for the current sample and the performed campaign here.

### Surface analysis after the experimental campaign

Photographs of the C12A7:e<sup>-</sup> sample before and after the conducted experimental campaign are depicted in Fig. 4, with front side denoting the plasma facing surface and rear side the surface that was directed towards the sample holder. Before the campaign, both sides of the sample exhibit a rough, homogeneous and black surface. During the campaign, a surface texture change was observed at a spot close to the center of the front side. *Ex situ* magnification of this area by means of an optical microscope shows a higher surface roughness and reveals smooth islands of molten-like structures. This surface texture might be a result of biasing with -84 V during hydrogen plasma exposure, which was done during one of the first pulses for about half an hour. In this case, short bright flashes in front of the sample surface could occasionally be observed, associated with a considerable increase of the bias current. Since the surface modification appeared in an area approximately where the work function measurements were taken, a synergistic

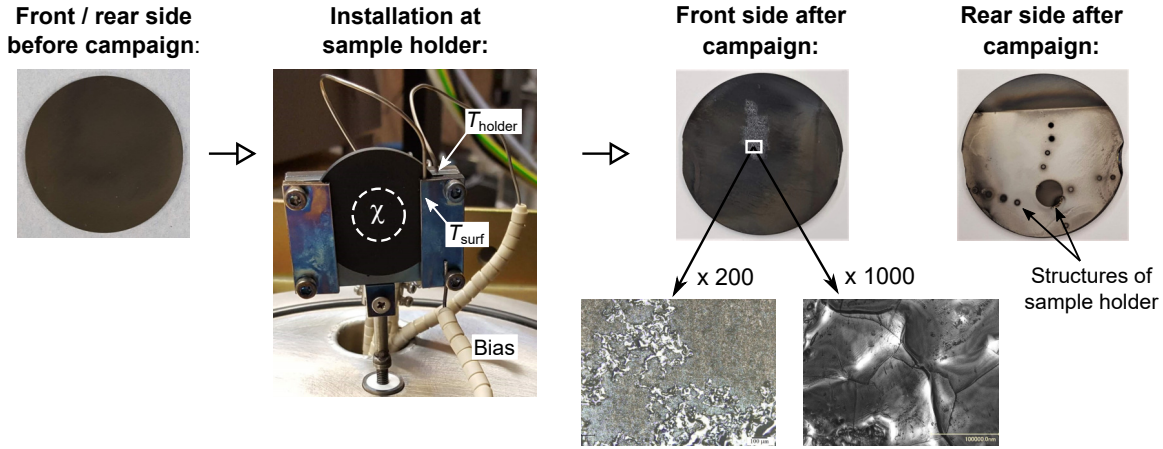


**FIGURE 4.** Photographs of the C12A7:e<sup>-</sup> sample before and after the conducted experiments, where the sample was clamped to a stainless steel sample holder in the plasma chamber. Front side denotes the surface which was exposed to plasma and rear side the surface which was directed towards the sample holder. The spot on the front side which was illuminated for measuring the work function  $\chi$  is indicated by a white dashed circle. The surface texture change on the front side after the campaign is magnified by means of an optical microscope.

interplay of UV irradiation, plasma irradiation and thermal effects in the presence of residual impurities might play a role. The occurrence of the surface change was already detected in the vacuum chamber by eye. In order to check a possible influence on the photoelectric response, the spot for the work function measurement was shifted. However, the photoelectric measurements did not change by shifting the observation area. Apart from the molten-like structures, the C12A7:e<sup>-</sup> surface has demonstrated good resilience to plasma exposure.

The surface which was in direct contact with the stainless steel sample holder, however, changed its color from black to whitish-brownish. Only the areas that were not in direct contact with the sample holder preserved the black coloration, which includes the upper part and spots where the holder provides holes for outgassing and diagnostic purposes. The color change indicates a degeneration of the electride surface state, which might be the result of an extensive heat treatment in direct contact with the stainless steel material and/or due to adsorbates from ambient air from before the installation of the sample. Further, some small pieces of the sample at the clamp positions flaked off, which is probably the result of thermal stress at elevated temperatures.

## SUMMARY AND CONCLUSIONS

The air-stable, mechanically robust and machinable C12A7 electride was investigated in view of a potential converter surface material for negative ion sources. The material has proven to be resilient to hydrogen and deuterium plasma exposure at ion source relevant conditions. After initial conditioning of the surface by thermal annealing and plasma exposure, short plasma pulses lead to a work function to  $\sim 3.2$  eV, and the application of a positive bias potential further lowers the work function to  $2.9 \pm 0.1$  eV. In contrast, the application of a negative bias potential leads to an increase of the work function and a strong decrease of the photoelectric yield of the surface. Thus, the flux ratio of positive ions to electrons onto the C12A7:e<sup>-</sup> surface determines the work function performance, which is presumably due to changes of the anionic electron density in the surface cages. It should be noted that at present-day test facilities, the caesiated plasma grid is biased positively with respect to the source body in order to reduce the co-extracted electrons [22].

The measured work function minimum of the tested C12A7:e<sup>-</sup> sample is about 0.5 eV higher than the intrinsic work function value for the chemically pure bulk in UHV. However, it has to be kept in mind that the material was placed in a  $10^{-6}$  mbar vacuum environment and the initial annealing took place with a sample holder temperature of 850 °C and a sample surface temperature of 570 °C in maximum. Furthermore, as described in [21], an extended long-term plasma exposure has a beneficial impact on the work function performance of the electride.

With regard to the state-of-the-art technique of *in situ* caesiation of metallic surfaces, work functions of about 2 eV are measured at the same experimental setup [23, 24]. Therefore, a smaller H<sup>-</sup> conversion yield via direct electron

transfer from the surface can be expected with the use of C12A7:e<sup>-</sup>. Nevertheless, other negative ion production channels may also be of importance, e.g., desorption of H<sup>-</sup> formed inside the surface cages in a hydrogen environment [25]. Consequently, the production of negative hydrogen ions directly above the C12A7:e<sup>-</sup> surface should be investigated. In a next step, an implementation at a test facility with an extraction system is desirable for a final conclusion on the C12A7 electride as Cs-free alternative, where the extracted negative ion current density together with the co-extracted electron current density can be investigated. Considering a plasma grid made of C12A7:e<sup>-</sup> in negative ion sources for fusion, points such as manufacturing a large surface area with a complex geometry, application of high temperatures for conditioning purposes and the application of a current through the grid for the generation of a magnetic filter field need to be addressed as well.

## ACKNOWLEDGMENTS

The authors would like to thank H. Hosono for the use of the C12A7 electride. The C12A7 electride was supplied from AGC Inc., and technical support by Naomichi Miyakawa, Satoru Watanabe and Kazuhiro Ito of AGC Inc. and discussion with them are greatly acknowledged. Furthermore, we would like to thank M. Wada for the *ex situ* investigations of the sample surface.

This work has been carried out within the framework of the EUROfusion Consortium and has received funding from the Euratom research and training programme 2014 – 2018 and 2019 – 2020 under grant agreement No 633053. The views and opinions expressed herein do not necessarily reflect those of the European Commission. Further, it was supported by Grant-in-Aid for Scientific Research of JSPS, 19H01883, 17H03512.

## REFERENCES

1. U. Fantz and J. Lettry, "Focus on sources of negatively charged ions," *New J. Phys.* **20**, 060201 (2018).
2. M. Bacal and M. Wada, "Negative hydrogen ion production mechanisms," *Appl. Phys. Rev.* **2**, 021305 (2015).
3. H. B. Michaelson, "The work function of the elements and its periodicity," *J. Appl. Phys.* **48**, 4729–4733 (1977).
4. U. Fantz, C. Hopf, R. Friedl, S. Cristofaro, B. Heinemann, S. Lishev, and A. Mimo, "Technology developments for a beam source of an NNBI system for DEMO," *Fusion Eng. Des.* **136**, 340–344 (2018).
5. U. Kurutz, R. Friedl, and U. Fantz, "Investigations on Cs-free alternatives for negative ion formation in a low pressure hydrogen discharge at ion source relevant parameters," *Plasma Phys. Control. Fusion* **59**, 075008 (2017).
6. R. Friedl, S. Cristofaro, and U. Fantz, "Work function of Cs-free materials for enhanced H<sup>-</sup> surface production," *AIP Conf. Proc.* **2011**, 050009 (2018).
7. D. Kogut, R. Moussaoui, N. Ning, J. B. Faure, J. M. Layet, T. Farley, J. Achard, A. Gicquel, and G. Cartry, "Impact of positive ion energy on carbon-surface production of negative ions in deuterium plasmas," *J. Phys. D: Appl. Phys.* **52**, 435201 (2019).
8. S. Matsuishi, Y. Toda, M. Miyakawa, K. Hayashi, T. Kamiya, M. Hirano, I. Tanaka, and H. Hosono, "High-Density Electron Anions in a Nanoporous Single Crystal: [Ca<sub>24</sub>Al<sub>28</sub>O<sub>64</sub>]<sup>4+</sup>(4e<sup>-</sup>)," *Science* **301**, 626–629 (2003).
9. H. Hosono, "Functioning of traditional ceramics 12CaO·7Al<sub>2</sub>O<sub>3</sub> utilizing built-in nano-porous structure," *Sci. Technol. Adv. Mater.* **5**, 409–416 (2004).
10. S. W. Kim and H. Hosono, "Synthesis and properties of 12CaO·7Al<sub>2</sub>O<sub>3</sub> electride: review of single crystal and thin film growth," *Phil. Mag.* **92**, 2596–2628 (2012).
11. Y. Toda, H. Yanagi, E. Ikenaga, J. J. Kim, M. Kobata, S. Ueda, T. Kamiya, M. Hirano, K. Kobayashi, and H. Hosono, "Work Function of a Room-Temperature, Stable Electride [Ca<sub>24</sub>Al<sub>28</sub>O<sub>64</sub>]<sup>4+</sup>(e<sup>-</sup>)<sub>4</sub>," *Adv. Mater.* **19**, 3564–3569 (2007).
12. Y. Toda, Y. Kubota, M. Hirano, H. Hirayama, and H. Hosono, "Surface of Room-Temperature-Stable Electride [Ca<sub>24</sub>Al<sub>28</sub>O<sub>64</sub>]<sup>4+</sup>(e<sup>-</sup>)<sub>4</sub>: Preparation and Its Characterization by Atomic-Resolution Scanning Tunneling Microscopy," *ACS Nano* **5**, 1907–1914 (2011).
13. H. Yanagi, T. Kuroda, K.-B. Kim, Y. Toda, T. Kamiya, and H. Hosono, "Electron injection barriers between air-stable electride with low work function, C12A7:e<sup>-</sup>, and pentacene, C<sub>60</sub> and copper phthalocyanine," *J. Mater. Chem.* **22**, 4278–4281 (2012).
14. R. Friedl and U. Fantz, "Influence of cesium on the plasma parameters in front of the plasma grid in sources for negative hydrogen ions," *AIP Conf. Proc.* **1515**, 255–262 (2013).
15. R. Friedl and U. Fantz, "Fundamental studies on the Cs dynamics under ion source conditions," *Rev. Sci. Instrum.* **85**, 02B109 (2014).
16. R. H. Fowler, "The Analysis of Photoelectric Sensitivity Curves for Clean Metals at Various Temperatures," *Phys. Rev.* **38**, 45–56 (1931).
17. T. E. Fischer, "Determination of semiconductor surface properties by means of photoelectric emission," *Surf. Sci.* **13**, 30–51 (1969).
18. P. Lange, D. Grider, H. Neff, J. K. Sass, and R. Unwin, "Limitations of the Fowler method in photoelectric work function determination: Oxygen on magnesium single crystal surfaces," *Surf. Sci. Lett.* **118**, L257–L262 (1982).
19. S. Briefi and U. Fantz, "Spectroscopic investigations of the ion source at BATMAN upgrade," *AIP Conf. Proc.* **2052**, 040005 (2018).
20. P. V. Sushko, A. L. Shluger, M. Hirano, and H. Hosono, "From Insulator to Electride: A Theoretical Model of Nanoporous Oxide 12CaO·7Al<sub>2</sub>O<sub>3</sub>," *J. Am. Chem. Soc.* **129**, 942–951 (2007).
21. A. Heiler, K. Waetzig, M. Tajmar, R. Friedl, R. Nocentini, and U. Fantz, "Work function performance of a C12A7 electride surface exposed to low pressure low temperature hydrogen plasmas," *J. Vac. Sci. Technol. A* **39**, 013002 (2021).

22. C. Wimmer, U. Fantz, and NNBI-Team, "Extraction of negative charges from an ion source: Transition from an electron repelling to an electron attracting plasma close to the extraction surface," *J. Appl. Phys.* **120**, 073301 (2016).
23. R. Friedl and U. Fantz, "Influence of H<sub>2</sub> and D<sub>2</sub> plasmas on the work function of caesiated materials," *J. Appl. Phys.* **122**, 083304 (2017).
24. S. Cristofaro, R. Friedl, and U. Fantz, "Correlation of Cs flux and work function of a converter surface during long plasma exposure for negative ion sources in view of ITER," *Plasma Res. Express* **2**, 035009 (2020).
25. M. Sasao, R. Moussaoui, D. Kogut, J. Ellis, G. Cartry, M. Wada, K. Tsumori, and H. Hosono, "Negative-hydrogen-ion production from a nanoporous 12CaO·7Al<sub>2</sub>O<sub>3</sub> electride surface," *Appl. Phys. Express* **11**, 066201 (2018).